STEM CELLS TRANSLATIONAL MEDICINE®

TISSUE-SPECIFIC PROGENITOR AND STEM CELLS

Intrastriatal Transplantation of Adult Human Neural Crest-Derived Stem Cells Improves Functional Outcome in Parkinsonian Rats

JANINE MÜLLER,[a,*] CHRISTIANA OSSIG,[b,c,*] JOHANNES F.W. GREINER,[d] STEFAN HAUSER,[a] MAREIKE FAUSER,[b,c] DARIUS WIDERA,[d] CHRISTIAN KALTSCHMIDT,[d] ALEXANDER STORCH,[b,c,*] BARBARA KALTSCHMIDT[a,d,*]

Key Words. Adult stem cells • Neural differentiation • Parkinson's disease • Cell transplantation • Nasal stem cells

[a]Molecular Neurobiology, University of Bielefeld, Bielefeld, Germany; [b]Division of Neurodegenerative Diseases, Department of Neurology, and Center for Regenerative Therapies Dresden, Dresden University of Technology, Dresden, Germany; [c]German Center for Neurodegenerative Diseases Dresden, Dresden, Germany; [d]Cell Biology, University of Bielefeld, Bielefeld, Germany

[*]Contributed equally.

Correspondence: Barbara Kaltschmidt, Ph.D., Universitätsstrasse 25, 33511 Bielefeld, Germany. Telephone: 49-521-106-5624; E-Mail: barbara.kaltschmidt@uni-bielefeld.de; or Alexander Storch, M.D., Fetscherstrasse 74, 01307 Dresden, Germany. Telephone: 49-(0)351-458-2532; E-Mail: Alexander.Storch@neuro.med.tu-dresden.de

Received April 7, 2014; accepted for publication October 21, 2014; first published online in SCTM *EXPRESS* December 5, 2014.

1066-5099/2014/$20.00/0

http://dx.doi.org/10.5966/sctm.2014-0078

ABSTRACT

Parkinson's disease (PD) is considered the second most frequent and one of the most severe neurodegenerative diseases, with dysfunctions of the motor system and with nonmotor symptoms such as depression and dementia. Compensation for the progressive loss of dopaminergic (DA) neurons during PD using current pharmacological treatment strategies is limited and remains challenging. Pluripotent stem cell-based regenerative medicine may offer a promising therapeutic alternative, although the medical application of human embryonic tissue and pluripotent stem cells is still a matter of ethical and practical debate. Addressing these challenges, the present study investigated the potential of adult human neural crest-derived stem cells derived from the inferior turbinate (ITSCs) transplanted into a parkinsonian rat model. Emphasizing their capability to give rise to nervous tissue, ITSCs isolated from the adult human nose efficiently differentiated into functional mature neurons in vitro. Additional successful dopaminergic differentiation of ITSCs was subsequently followed by their transplantation into a unilaterally lesioned 6-hydroxydopamine rat PD model. Transplantation of predifferentiated or undifferentiated ITSCs led to robust restoration of rotational behavior, accompanied by significant recovery of DA neurons within the substantia nigra. ITSCs were further shown to migrate extensively in loose streams primarily toward the posterior direction as far as to the midbrain region, at which point they were able to differentiate into DA neurons within the locus ceruleus. We demonstrate, for the first time, that adult human ITSCs are capable of functionally recovering a PD rat model. STEM CELLS TRANSLATIONAL MEDICINE *2015;4:31–43*

INTRODUCTION

Parkinson's disease (PD) is considered one of the most severe neurodegenerative diseases. PD results in dysfunctions of the motor system such as resting tremor, rigidity, and bradykinesia and in nonmotor symptoms such as depression. Affecting up to 2% of the population aged >60 years in industrialized countries and 3%–4% of people aged >80 years [1, 2], PD is also the second most frequent neurodegenerative disease.

Symptoms observed during PD are closely associated with a progressive loss of dopamine (DA) neurons within the substantia nigra (SN) [3]. In this regard, therapeutic strategies mainly include the pharmacological administration of levodopa [4] or deep brain stimulation [5, 6] and the application of neurotrophic factors [7] or gene therapy [8], both of which are currently in clinical studies. Notably, such therapeutic strategies are still limited in terms of motor complications (e.g., levodopa-induced dyskinesias) [9], hallucinations, and reduced response to pharmacological treatment over time [10].

Addressing these challenges, cell replacement therapy aims to restore DA neurons lost during the disease rather than solely fight its symptoms. Besides fetal DA neuron-based approaches [11–14], Kriks and colleagues demonstrated behavioral recovery of parkinsonian mice, rats, and monkeys after transplantation of predifferentiated human embryonic stem cells (ESCs) [15]. However, medical applications of human ESCs are still a matter of ethical and practical considerations, particularly in terms of their potential tumorigenicity [16–19].

Contemplating these aspects, stem cells residing within the adult human body remain a promising tool for treating PD. Although restricted in their differentiation potential, these stem cells possess the capability to self-renew and give rise to multiple specialized cell types [20], thereby exhibiting remarkably low tumorigenicity [16, 18, 21, 22]. Another advantage of adult stem cells is that their application allows autologous cell transplantation,

avoiding the need for long-term immunosuppression in the patient [23–26]. With respect to PD treatment strategies, rat mesenchymal stem cells (MSCs) were recently reported to differentiate into tyrosine hydroxylase-positive (TH^+) DA neurons in a 6-hydroxydopamine (6-OHDA) rat model, accompanied by slight improvement of motor deficits after 8 weeks [27]. Transferring these promising findings to the human system, human MSCs were also proposed to undergo differentiation into DA neuron-like cells [28, 29]. However, the functionality of respective neuron-like cells is still a matter of debate [30].

During the past decade, several neural crest-derived stem cell (NCSC) sources were identified within craniofacial tissue, including hair [31–33], hard palate [34], oral mucosa [35, 36], or periodontal ligament [37, 38] (reviewed in [39]). In 2012, we reported the successful isolation of NCSCs from the respiratory mucosa of the human inferior turbinate. In addition to their high plasticity, NCSCs derived from adult inferior turbinate tissue (ITSCs) could be easily obtained and efficiently cultivated and thus potentially used in autologous approaches ([40–42]). Given these characteristics, ITSCs appear to be promising candidates for potential autologous cell-replacement therapies.

NCSCs have been widely shown to sufficiently undergo differentiation into the ectodermal lineage [32, 36, 43], emphasizing their potential to treat neurodegenerative disorders. Notably, NCSCs from mammalian dermis were also shown to give rise to DA neuron-like cells via application of a synthetic peptide derived from von Hippel-Lindau protein [44]. Very recently, Sieber-Blum et al. additionally reported the successful differentiation of human epidermal NCSCs into functional dopaminergic neurons in vitro [45].

Extending these promising findings, we assessed the potential of adult human NCSCs for treating PD using a parkinsonian rat model. Prior to investigations in vivo, ITSCs were shown to efficiently undergo differentiation into mature functional neurons in vitro. To further demonstrate their potential to recover nervous tissue, we achieved successful predopaminergic differentiation of ITSCs by activating the sonic hedgehog (SHH) pathway. Notably, transplantation of pre- or undifferentiated ITSCs into the striatum of unilaterally lesioned 6-OHDA rats led to restored rotational behavior. Behavioral improvement was further shown to be accompanied by significant recovery of TH-positive DA neuron populations within the SN. Although surviving ITSCs were located between the transplantation site and the SN, we also observed the presence of DA neurons of human origin in the locus ceruleus. Our findings suggest a beneficial role for ITSCs in the observed behavioral recovery, emphasizing their promising potential for future treatment of PD.

Materials and Methods

Isolation and Cultivation of ITSCs

ITSCs were isolated from adult human inferior turbinate tissue and precultivated, as described previously [41]. The cultures were grown in serum-free medium consisting of Dulbecco's modified Eagle's medium/Ham F-12 (DMEM/F-12; Biochrom, Berlin, Germany, http://www.biochrom.de) supplemented with basic fibroblast growth factor-2 (FGF2; 40 ng/ml; made in the laboratory), epidermal growth factor (EGF; 20 ng/ml; R&D Systems, MN, http://www.rndsystems.com), 0.5 U/ml heparin (catalog no. H3149; Sigma-Aldrich, Schnelldorf, Germany, http://www.sigmaaldrich.com), and 3× B27 supplement (made in the laboratory). Neurospheres were dissociated using collagenase I (NB 4; 0.3 U/ml, 90 minutes at 37°C; Serva Electrophoresis, Heidelberg, Germany, http://www.serva.de).

Neural Differentiation of ITSCs

ITSCs were cultivated in serum-free medium, as described above, for 2 days. Neurospheres were dissociated using collagenase I (NB 4; 0.3 U/ml, 90 minutes at 37°C; Serva Electrophoresis). Dissociated cells were resuspended in DMEM high glucose (PAA Laboratories, Pasching, Austria, http://www.paa.at) containing 200 mM L-glutamine (Sigma-Aldrich) and 10% fetal calf serum (FCS; lot 126K3398; Sigma-Aldrich) and plated at a density of 4×10^5 cells per well (12-well plate), followed by cultivation at 37°C, 5% CO_2 and atmospheric O_2 in a humidified incubator (Binder, Tuttlingen, Germany, http://www.binder-world.com/en/) for at least 2 days. Subsequently, the medium was changed to a neuronal induction medium (NIM) containing DMEM high glucose, 200 mM L-glutamine, 10% FCS (lot 126K3398), 500 μM 3-isobutyl-1-methylxanthine, 200 μM indomethacin, 1 μM dexamethasone, and 2 μM insulin (all from Sigma-Aldrich). After 7 days, maturation of ITSCs was achieved by adding 0.5 μM retinoic acid (Sigma-Aldrich) and 1× N-2 supplement (Gibco, Darmstadt, Germany, http://www.invitrogen.com). The medium was changed by removing half of the medium volume, followed by addition of fresh prewarmed NIM containing 1× N-2 supplement (Life Technologies, Darmstadt, Germany, http://www.lifetech.com).

Glial Differentiation of ITSCs

For coculture, mouse astrocytes were prepared from cortex of postnatal day 1 (P1) C57BL/6 mice. Brain tissue was incubated with 1× trypsin/EDTA (PAA Laboratories) for 15–30 minutes at 37°C. Astrocytes were washed with prewarmed DMEM (37°C; Sigma-Aldrich) and transferred to DMEM containing 2 mM L-glutamine, 100 U/ml penicillin and streptomycin, and 10% FCS (Sigma-Aldrich). Confluent astrocyte cultures were treated with mitomycin C (10 μg/ml; Sigma-Aldrich) for 2 hours to eliminate proliferating cells, followed by replacement of medium to prewarmed fresh medium for 24 hours. Inactivated astrocytes were seeded at 80% confluence to 12-well plates containing paraffin blocks to ensure a noncontact coculture. ITSCs seeded on glass coverslips (diameter, 18 mm; R. Langenbrinck, Emmendingen, Germany, http://www.langenbrinck.com) at a density of 1×10^5 cells were placed on top of paraffin blocks. Cocultures were further cultivated in DMEM containing 1% FCS at 37°C and 5% CO_2 for 14 days.

Predopaminergic Differentiation

Dissociated secondary neurospheres were resuspended in serum-free medium consisting of DMEM/F-12 (Biochrom) supplemented with FGF2 (40 ng/ml), EGF (20 ng/ml; R&D Systems), heparin (2 mg/ml; Sigma-Aldrich), and B27 supplement and plated on poly-D-lysine/laminin-coated 6-well plates. After 24 hours, different concentrations of purmorphamine (0.1, 0.5, 1, 5, or 10 μM; Enzo Life Sciences GmbH, Lörrach, Germany, http://www.enzolifesciences.com) or sonic hedgehog (200 ng/ml; Peprotech, Hamburg, Germany, http://www.peprotech.com) were added to the medium. After 48 hours, cDNA synthesis followed by quantitative polymerase chain reaction (qPCR) was performed, as described below.

Dopaminergic Differentiation

ITSCs were cultivated in serum-free medium, as described above, for 2 days. Subsequently, neurospheres were dissociated using collagenase I. For dopaminergic differentiation, the protocol recently described by Sieber-Blum et al. [45] was applied with slight modifications. Moreover, 5×10^4 cells were seeded on 8-mm uncoated glass coverslips and cultivated for 12 hours in DMEM high glucose supplemented with 10% FCS. For induction, cultures were exposed to DMEM high glucose supplemented with 1% FCS, penicillin/streptomycin, β-mercaptoethanol (10 μM), B27 without retinoic acid (1×; Life Technologies), purmorphamine (10 μM; Sigma-Aldrich), FGF8 (100 ng/ml; Peprotech), recombinant human glial cell line-derived neurotrophic factor (GDNF; 5 ng/ml; Peprotech), recombinant human brain-derived neurotrophic factor (BDNF; 20 ng/ml; Peprotech), nerve growth factor (NGF; 20 ng/ml; Peprotech), dibutyryl cAMP (1 mM; Sigma-Aldrich), ascorbic acid (200 μM; Sigma-Aldrich), SB-431542 (10 μM; Sigma-Aldrich), LDN 193189 (100 nM; Abcam, Cambridge, U.K. , http://www.abcam.com), and CHIR99021 (0.5 μM; Abcam). CHIR99021 was removed after 24 hours. On day 4 of differentiation, the WNT inhibitor IWP-4 (Miltenyi Biotec, Bergisch Gladbach, Germany, http://www.miltenyibiotec.com) was added to the media at a concentration of 100 nM, which was increased to 1 μM at day 6 of differentiation, followed by withdrawal of FCS at day 7. At day 9, the concentration of purmorphamine was decreased to 5 μM. Medium was replaced with prewarmed fresh medium daily.

Reverse Transcription-Polymerase Chain Reaction

Total RNA was isolated using RNeasy Mini Kit (Qiagen, Hilden, Germany, http://www.qiagen.com), according to the manufacturer's guidelines. Quality and concentration of isolated RNA was subsequently investigated by Nanodrop ultraviolet spectrophotometry. Afterward, cDNA was synthesized using the First Strand cDNA Synthesis Kit (Fermentas Life Sciences, St. Leon-Rot, Germany, http://www.fermentas.com). Polymerase chain reaction (PCR) was performed using the KAPA2G Robust PCR Kit (Peqlab Biotechnology, Erlangen, Germany, http://www.peqlab.de/wcms/en/index.php).

qPCR

All qPCRs were performed in triplicate using Platinum SYBR Green qPCR SuperMix-UDG (Invitrogen, Carlsbad, CA, http://www.invitrogen.com; Life Technologies), according to the manufacturer's guidelines, and assayed with a Rotor-Gene 6000 (Qiagen).

Immunocytochemistry

Differentiated ITSCs were fixed in phosphate-buffered 4% paraformaldehyde (PFA; pH 7.4; 4% wt/vol paraformaldehyde, 100 mM NaH_2PO_4, 0.4 mM $CaCl_2$) for 20 minutes at room temperature (RT) followed by 3 wash steps in 1× phosphate-buffered saline (PBS) for 5 minutes. The cells were permeabilized with 0.02% Triton X-100 for 30 minutes at RT and blocked using 5% of appropriate serum, followed by incubation with primary antibodies for 1 hour at RT. Antibodies used were anti-βIII-tubulin (Promega, Mannheim, Germany, http://www.promega.com), anti-neurofilament NF200 (Sigma-Aldrich), anti-Map2 (Millipore, Billerica, MA, http://www.millipore.com), anti-synaptophysin (Millipore), anti-GFAP (BD Bioscience, Heidelberg, Germany, http://www.bdbiosciences.com), anti-Pitx3 (Millipore), and anti-TH (Santa Cruz Biotechnology, Heidelberg, Germany, http://www.scbt.com). The secondary fluorochrome-conjugated antibodies (Alexa 555 and Alexa 488; Life Technologies) were incubated for 1 hour at RT. Nuclear counterstaining was performed with SYTOX green (1:20,000; Molecular Probes, Göttingen, Germany, http://probes.invitrogen.com), 4′,6-diamidino-2-phenylindole (DAPI; 0.5 μg/ml; Sigma-Aldrich), or TOTO-3 iodide (642/660 nm; Life Technologies). Fluorescence imaging was performed using a confocal laser scanning microscopy (LSM 510 or LSM 780; Carl Zeiss, Jena, Germany, http://www.zeiss.com) and analyzed using ZEN software from the same provider.

Vesicle Recycling

Detection of vesicle recycling was analyzed in directly differentiated and spontaneously differentiated ITSCs using FM 1-43FX lipophilic styryl dye (Life Technologies, Molecular Probes), according to the manufacturer's guidelines. In particular, cells were washed in Hanks' balanced saline solution (Sigma-Aldrich), stimulated with 75 mM KCl, and stained for 90 seconds with FM 1-43FX dye. Fluorescence imaging was performed using fluorescence microscopy (Observer D1; Carl Zeiss).

Calcium Imaging

Differentiated ITSCs were loaded with the calcium indicator dye Fluo-4 AM (Invitrogen) for 30 minutes at 37°C. To reduce leakage of the de-esterified indicator, 1 mM probenecid was added to the staining solution. Cells were washed 3 times with Ringer's solution (made in the laboratory) and incubated 30 minutes at 37°C to allow complete de-esterification of intracellular AM esters. Cells growing on a glass coverslip were clamped on a custom-made imaging chamber and rinsed with Ringer's solution. Stimulation was achieved by changing the potassium concentration of the Ringer's solution to a final concentration of 75 mM KCl. Ca^{2+} measurement was performed using detection of Fluo-4 fluorescence using fluorescence microscopy (Observer D1; Carl Zeiss).

6-OHDA-Lesioned Rats

Female Wistar rats (~240 g at purchase; Janvier Labs, Saint-Berthevin Cedex, France, http://www.janvier-labs.com) were maintained under a 12-hour light/dark cycle with constant temperature and humidity. Food and water were available ad libitum. All animal work was performed in accordance with regulations set by the ethical committee for the use of laboratory animals at Dresden University of Technology in Germany. The ascending DA pathways on the right side were lesioned with 6-OHDA (Sigma-Aldrich) to generate a stable hemiparkinsonian phenotype [46]. Prior to surgery, animals were anesthetized using isoflurane and O_2. All rats received stereotactic injections unilaterally into the medial forebrain bundle to target the nigrostriatal tract. Lesion was achieved with 6-OHDA (3.6 mg/ml in 0.2 mg ascorbate per milliliter of 0.9% NaCl) using a two-track protocol: track 1: tooth bar (TB) −2.3, anteroposterior (AP) −4.4, lateral (L) −1.2, dorsoventral (DV) −7.8; track 2: TB +3.4, AP−4.0, L−0.8, DV−8.0. The total volume injected per animal was 5.5 μl (2.5 μl in the first track and 3 μl in the second track; 19.8 μg per animal). The rate of injection was 1 μl/minute, and the

cannula was left in place for 4 minutes before retracting to prevent backflow.

Transplantation Procedure

Well-lesioned animals were divided into three groups to receive ITSCs cultured in standard medium, ITSCs pretreated with SHH/FGF8 (SHH 200 ng/ml, FGF8 100 ng/ml for 2 days; Peprotech) or saline as a sham control. Transplantation was performed 6 weeks after lesioning. Overall, 500,000 cells were stereotactically implanted into the striatum of anesthetized animals via a 10-μl Hamilton syringe at the following coordinates in the striatum ipsilateral to the 6-OHDA lesion: TB 0.0 mm, AP +0.2 mm, L −3.5 mm. Two 2.5-μl deposits were injected at DV −5.0 mm and −4.0 mm, and the needle was kept in place for an additional 4 minutes before it was slowly retracted. Animals received daily injections of cyclosporin A i.p. for immunosuppression (1 ml/kg body weight; 5 ml of cyclosporin A dissolved in 20 ml of 0.9% saline; liquid from Novartis, Nürnberg, Germany, http://www.novartis.com) until perfusion. To prevent infections, all animals received Trimetox 240 (sulfadoxine 200 mg/ml, trimethoprim 40 mg/ml; Veyx Pharma, Schwarzenborn, Germany, http://www.veyx.de/en/int/veyx-pharma/) daily via the drinking water (50–75 mg/kg body weight).

Amphetamine-Induced Rotational Behavior

Amphetamine-induced rotations were carried out to functionally assess the DA system [47]. Baseline measures were obtained 4 weeks following 6-OHDA lesioning. Animals received an i.p. injection of 5.0 mg/kg body weight of amphetamine (Sigma-Aldrich) dissolved in saline and were placed in cylindrical bowls in which rotational behavior was observed and quantified by a rotometer system (Omnitech Electronics, Inc., Columbus, OH, http://www.omnitech-electronics.com). Rotational behavior was assessed for 90 minutes after injection. One full rotation was defined as 4 consecutive 90° turns in the same direction [48]. Animals meeting the criterion of $\geq$10 turns per minute (averaged over 90 minutes) were assigned to the transplant groups. Behavioral assessment was repeated 4, 8, and 12 weeks after grafting.

Immunohistochemistry

After 12 weeks, animals received i.p. injection of Rompun (0.1 ml, 20 mg/ml; Bayer-Germany) and ketamine (0.9 ml, 50 mg/ml; Parke-Davis [India] Ltd., Mumbai, India, , http://www.pfizer.com) and were transcardiacally perfused with 150 ml PBS followed by 300 ml PFA (4% in phosphate-buffered saline, pH 7.4). The brains were carefully removed and stored for 24 hours in PFA and afterward in 30% sucrose in PBS for cryoprotection. Afterward, the brains were frozen at −80°C before undergoing further analysis.

For immunohistochemistry, 40-μm-thick sagittal sections of rat brains were prepared. The sections were preincubated in 1× Tris-buffered saline (TBS) containing 0.5% Triton-X-100 and 5% respective serum (TBS+) for about 1 hour, followed by incubation with the primary antibodies in 1× TBS+ overnight at 4°C. Antibodies used were mouse anti-human STEM121 (StemCells, Inc., Cambridge, U.K., http://www.stemcellsinc.com), mouse anti-human nestin (Millipore), rabbit anti-TH (Santa Cruz Biotechnology Inc.), rabbit anti-Map2 (Millipore), rabbit anti-GFAP (BD Bioscience), and rabbit anti-Ki67 (Abcam). The sections were washed 3 times with 1× TBS for 15 minutes, incubated with the appropriate secondary fluorochrome-conjugated antibodies (Alexa 555, Alexa 488; Life Technologies) under exclusion of light for 2 hours, and washed another 3 times with 1× TBS. Nuclear counterstaining was performed with DAPI (0.5 μg/ml; Sigma-Aldrich) for 15 minutes. After staining, sections were washed 2 times, once with TBS and once with double-distilled water, and finally transferred on microscope slides for further analysis. Fluorescence imaging was carried out using a confocal laser scanning microscope (LSM 780; Carl Zeiss).

Nissl Staining

The 40-μm-thick sagittal sections of rat brains removed after 12 weeks and treated as described above were applied to 1% cresyl violet at 60°C for 15 minutes. Dehydration was performed afterward using 70%, 90%, and 100% ethanol for 3 minutes each, followed by clearing with xylene for 3 minutes. Sections were embedded in Entellan.

Imaging was done via light microscopy using an AMG EVOS xl microscope (PeqLab Biotechnology).

Cell Counting and Statistics

Stereologic counting of TH-positive cells was performed with the optical fractionator method using Stereoinvestigator software version 5.05.1 (MicroBrightField, Magdeburg, Germany), as described previously [49]. Images for counting were acquired using a 40× oil immersion, 1.3 numerical aperture objective on a Zeiss Axioplan 2 microscope equipped with a computer-controlled motorized three-dimensional stage (Ludel Electronic Products) and a video camera (MBF Bioscience CX9000, Williston, USA). Cells were counted if the upper top of the nucleus could be identified unequivocally. Statistical analyses were performed using SPSS software version 21.0 (IBM Corp, Armonk, NY, http://www-01.ibm.com/software/analytics/spss/). Statistical analysis was performed using an unpaired two-sided *t* test (comparing two groups), one-way analysis of variance (ANOVA) with post hoc Bonferroni-adjusted *t* test (comparing multiple groups), or two-way repeated-measure ANOVA with post hoc Bonferroni-adjusted *t* test for the behavioral data (comparing multiple groups over time). We applied various linear and nonlinear regression analyses, and logarithm function nicely matched the ipsilateral net rotations at 12 weeks and TH^+ cell count and rendered a correlation coefficient (r^2) of 0.687. Curve linearization was thus made by log transformation of results. Correlation analyses to assess the association of behavioral outcome and TH^+ DA neuron counts were performed by Pearson correlation test. If not mentioned otherwise, all data are displayed as mean ± SEM. The significance level was set at $p < .05$ (two-sided test).

To quantify fluorescence intensity of TH^+ fibers within the striatum, ImageJ was applied [50], followed by statistical analyses using GraphPad Prism (GraphPad Software, La Jolla, CA, http://www.graphpad.com). The *p* values were calculated by one-way ANOVA with post hoc Bonferroni-adjusted *t* test.

RESULTS

Neural Crest-Derived Stem Cells From Human Inferior Turbinate Are Able to Differentiate Efficiently Into the Neural Lineage In Vitro

Assessing their potential to give rise to neuronal tissue, we initially investigated the ability of human inferior turbinate stem

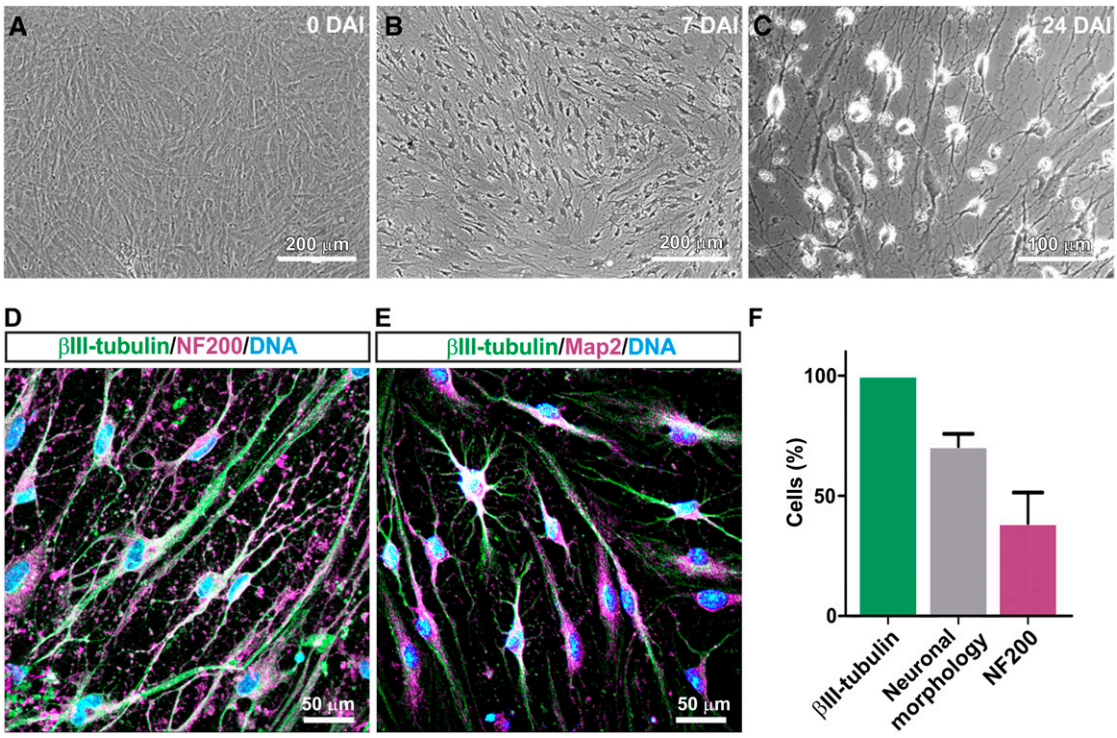

Figure 1. Adult human neural crest-derived stem cells derived from the inferior turbinate (ITSCs) are able to efficiently differentiate into the neural lineage. **(A):** High-cell-density monolayer was cultivated under exposure to a neuronal induction medium. **(B):** At 7 days after induction, most cells exhibited a neuronal morphology. **(C):** By differentiation day 24, cells had built up a dense neuronal network. **(D):** Immunocytochemical staining showed coexpression of βIII-tubulin and neurofilament (NF200) and **(E)** βIII-tubulin and Map2 at day 24 of differentiation. **(F):** Quantification of immunocytochemical analyses 24 days after induction; βIII-tubulin: 100% of analyzed cells; neuronal morphology: 70.7 $\pm$ 5.1% of βIII-tubulin-positive cells, NF200: 39% $\pm$ 10.3% of ITSCs showing neuronal morphology and expression of βIII-tubulin. Abbreviation: DAI, days after induction.

cells to undergo differentiation into the neural lineage in vitro. During exposure to a NIM, the cytoplasm of ITSCs was observed to retract toward the nucleus, followed by an enhanced neurite outgrowth accompanied by the formation of a dense neuronal network (Fig. 1A–1C). After 24 days of NIM treatment, immunocytochemical staining revealed expression of βIII-tubulin (100%) in ITSC-derived neuron-like cells, which also exhibited a neuronal morphology (70.7% $\pm$ 5.1% of βIII-tubulin-positive cells). We further observed the presence of mature neuronal marker neurofilament (39% $\pm$ 10.3% of ITSCs showing neuronal morphology and expression of βIII-tubulin) as well as Map2 at the protein level (Fig. 1D–1F). A small subpopulation of differentiated ITSCs expressed βIII-tubulin without possessing a neuronal morphology, suggesting them to be early neural progenitors. In addition, ITSCs cocultured with mouse astrocytes gave rise to 5.2% $\pm$ 1.0% of GFAP-positive glial cells (supplemental online Fig. 1), conclusively indicating the ability of ITSCs to differentiate into the neural lineage, including neurons and glia.

Synaptic Vesicle Recycling and Repeated Calcium Spiking Suggest Functionality of ITSC-Derived Neurons

In order to determine their functionality, neurons generated from ITSCs were analyzed for the release and uptake of neurotransmitters. As a crucial prerequisite for neurotransmitter-mediated signaling, ITSC-derived neurons possessed synaptophysin-positive synapses (Fig. 2B). Reverse transcription-PCR analyses further confirmed the expression of synaptophysin in differentiated ITSCs. Notably, the message for synaptophysin was observed to be strongly increased in ITSCs exposed to NIM in comparison with FCS control (Fig. 2A).

We further investigated potential recycling of synaptic vesicles in ITSC-derived neurons. After stimulation with 75 mM KCl, 33% $\pm$ 7.8% of the neurons generated from ITSCs showed incorporation of the fluorescent dye FM 1-43FX, indicating functional vesicle recycling (Fig. 2C; supplemental online Fig. 2). In contrast, undifferentiated ITSCs revealed no vesicle-mediated FM 1-43FX uptake (supplemental online Fig. 2). As a further hallmark of neuronal excitability, exocytosis of synaptic vesicles on depolarization is followed by calcium influx. We investigated potential changes in intracellular calcium concentration via intensity of Fluo-4 fluorescence on KCl-dependent stimulation. ITSC-derived neurons (Fig. 2D) showed repeated calcium spikes after respective restimulation (Fig. 2E, 2F), again indicating their functionality.

ITSCs Give Rise to TH$^+$ DA Neurons In Vitro

With respect to their potential application in a parkinsonian rat model, we initially investigated the ability of ITSCs to undergo predopaminergic differentiation in vitro prior to transplantation. Being an essential prerequisite for induction of a DA fate [51, 52], ITSCs showed activation of the hedgehog pathway in vitro after treatment with SHH or its agonist purmorphamine (Fig. 3A). In

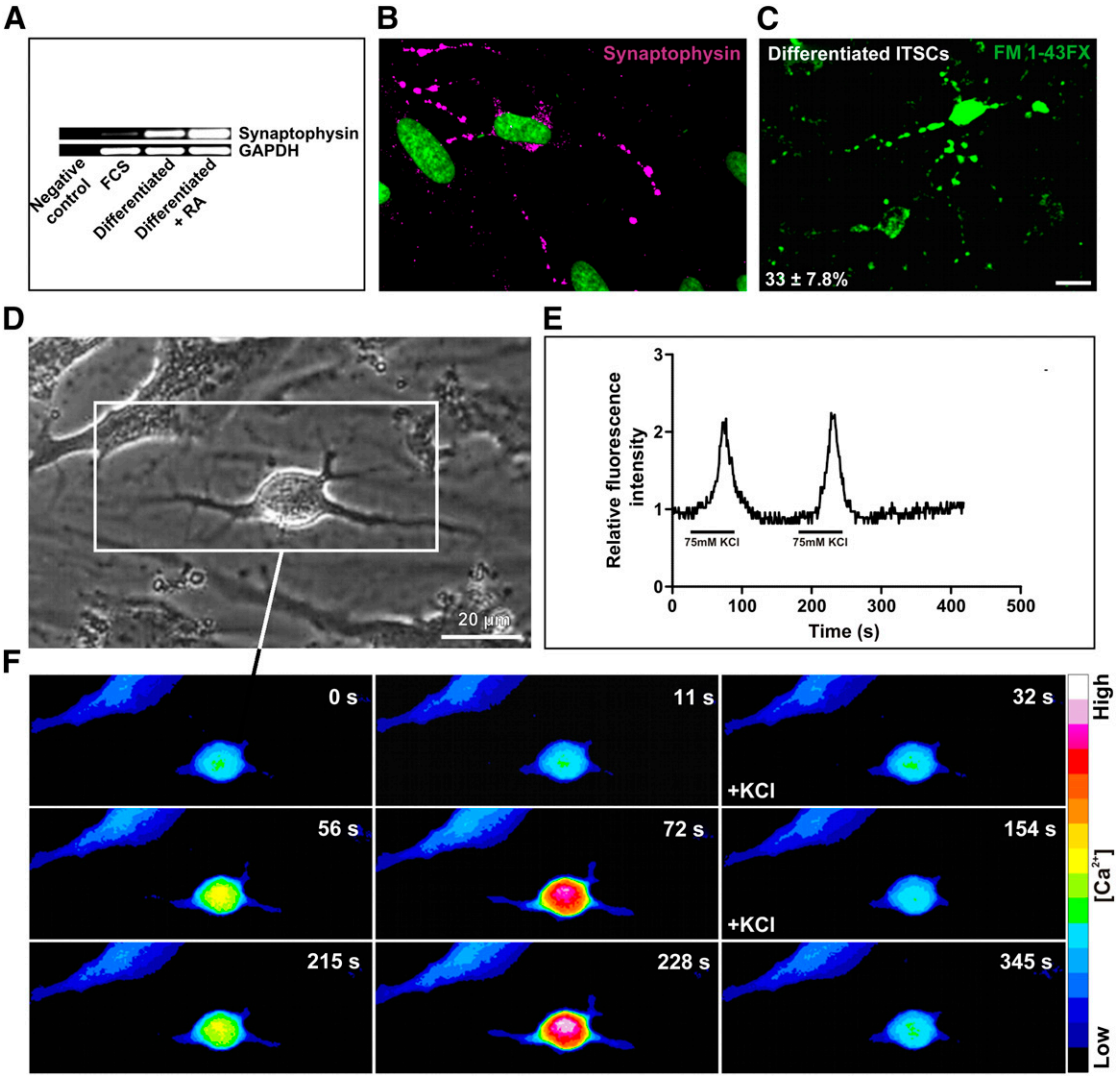

Figure 2. Chemical stimulation of ITSC-derived neurons led to synaptic vesicle recycling and repeated calcium spikes. **(A, B):** After neuronal induction medium-dependent differentiation, ITSC-derived neuronal cells revealed the presence of synaptophysin at the protein level and at the mRNA level. Treatment of neuronal culture with retinoic acid led to increased synaptophysin mRNA in contrast to spontaneous differentiation with FCS. Neurospheres served as a control. **(C):** After chemical stimulation with 75 mM KCl, cells that had differentiated for 14 days were able to internalize the fluorescent dye FM 1-43FX by vesicle uptake. Scale bar = 50 μM. **(D):** Neuronally differentiated cell subjected to calcium imaging. **(E):** Cells were subjected for 70 seconds to KCl. Stimulation with 75 mM KCl resulted in repeated calcium spikes. After washout of the stimulus and restimulation for 70 seconds, relative fluorescence intensity F/F0 was determined in three independent cells. **(F):** The sequential series of images of a neuronal cell showed that chemical stimulation induced an increase in fluorescence of the Ca^{2+}-sensitive indicator. Abbreviations: FCS, fetal calf serum; ITSCs, adult human neural crest-derived stem cells derived from the inferior turbinate; RA, retinoic acid; s, seconds.

order to differentiate ITSCs toward a more mature dopaminergic phenotype, we applied FGF8 and purmorphamine treatment in combination with dual SMAD inhibition and inhibited WNT signaling. In contrast to the FCS-treated control approach, directed dopaminergic differentiation of ITSCs for 12 days resulted in a population of 100% Pitx3-positive ITSC-derived dopaminergic progenitors coexpressing βIII-tubulin (Fig. 3B). Notably, although spontaneously differentiated ITSCs lacked expression of tyrosine hydroxylase, ITSCs that differentiated into the dopaminergic phenotype were positive for TH in the perinuclear area (Fig. 3C). ITSCs further showed expression of TH in the soma and in processes after dopaminergic differentiation for 20 days, indicating successful differentiation of ITSCs into DA neurons (Fig. 3D). In addition, we observed increased expression of Pitx3 in ITSCs after 30 days of differentiation in comparison with undifferentiated control using qPCR (Fig. 3E).

Transplantation of ITSCs Into 6-OHDA-Lesioned Parkinsonian Rats Leads to Behavioral Recovery

In order to assess potential functional effects of ITSCs, a parkinsonian rat model was established by unilaterally injecting 6-OHDA into the medial forebrain bundle. Four weeks after 6-OHDA injection, undifferentiated or SHH/FGF8-pretreated ITSCs were transplanted into the striatum ipsilateral to the lesioned site. Before transplantation, all rats exhibited severe motor asymmetry that was induced by amphetamine and that did not improve in sham control animals over time (Fig. 4). In contrast, rats transplanted

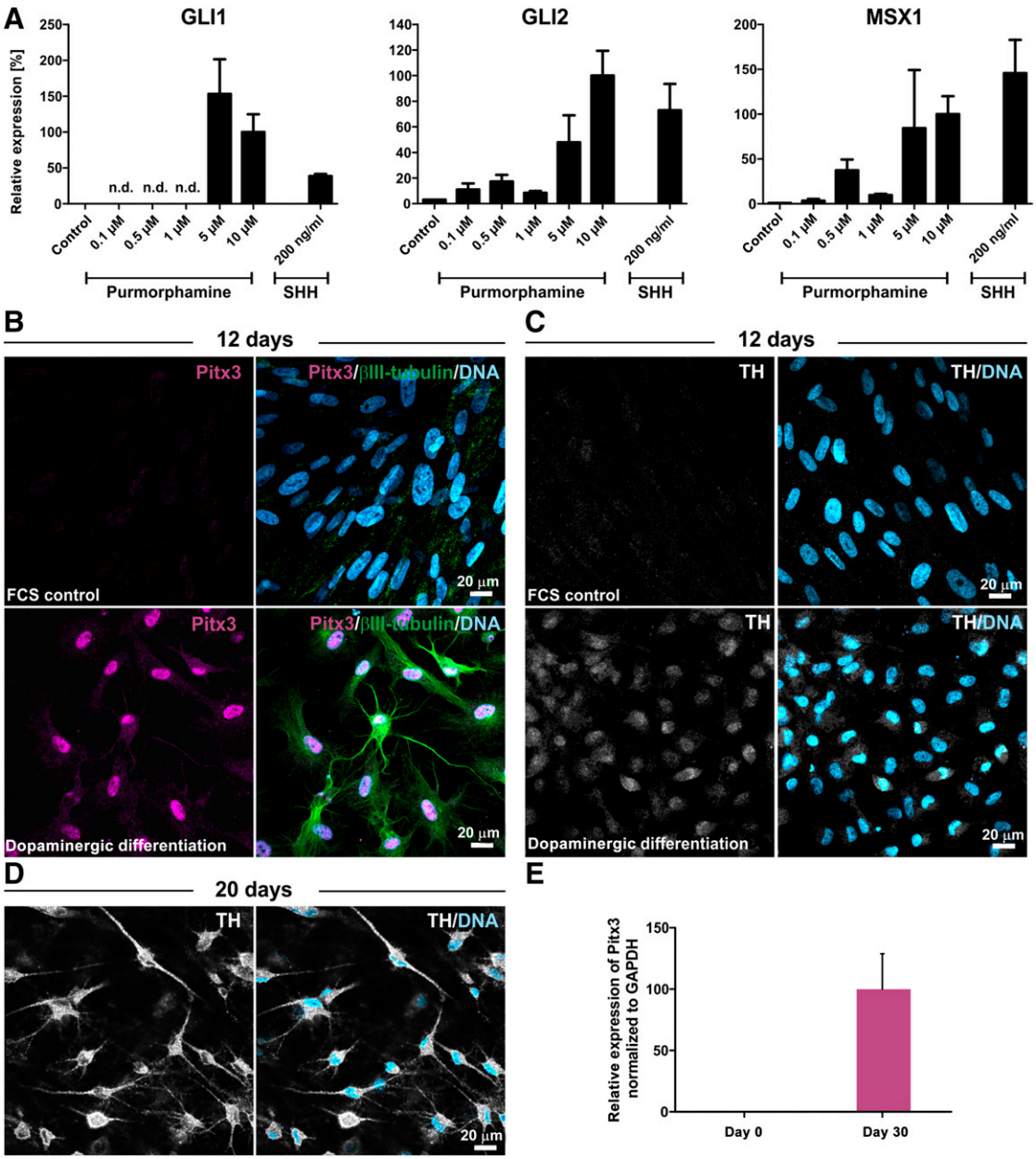

Figure 3. Adult human neural crest-derived stem cells derived from the inferior turbinate (ITSCs) give rise to TH$^+$ dopaminergic neurons in vitro. **(A):** Increased expression of the target genes Gli1, Gli2, and Msx1 after addition of purmorphamine or SHH shows activation of the hedgehog pathway in ITSCs. **(B):** In contrast to spontaneous differentiation, dopaminergic differentiation of ITSCs for 12 days resulted in dopaminergic progenitors coexpressing Pitx3 and βIII-tubulin. **(C):** Whereas spontaneously differentiated ITSCs lacked TH expression, ITSC-derived dopaminergic progenitors expressed TH in the perinuclear area. **(D):** Expression of TH in the soma and in processes of ITSC-derived dopaminergic neurons after dopaminergic differentiation for 20 days. **(E):** Quantitative polymerase chain reaction revealed increased expression of Pitx3 in ITSCs after 30 days of differentiation in comparison with undifferentiated controls. Abbreviations: FCS, fetal calf serum; n.d., no data; TH, tyrosine hydroxylase.

with undifferentiated ITSCs showed a progressive and strong reduction of ipsilateral amphetamine-induced rotations over the 12-week observation period (Fig. 4). The number of rotations was significantly lower compared with the control group at all observational time points after surgery. We likewise observed up to ~40% reduced rotations in rats transplanted with SHH/FGF8-pretreated ITSCs compared with the sham group, with no relevant differences to the undifferentiated ITSC-transplanted animal group (Fig. 4).

Lesioned Substantia Nigra of 6-OHDA-Treated Rats Is Restored After ITSC Transplantation

Investigating the observed behavioral recovery of 6-OHDA-lesioned rats in more detail, SN and striata were analyzed by immunohistochemistry 12 weeks after ITSC transplantation (Fig. 5). Hemispheres located contralateral to the site of 6-OHDA injection and ITSC transplantation were normal, with intact populations of TH$^+$ DA neurons (Fig. 5A, 5D; supplemental online Fig. 3). Notably,

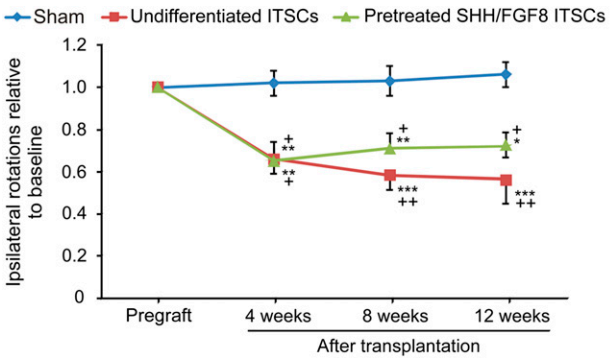

Figure 4. Transplantation of ITSCs into 6-hydroxydopamine (6-OHDA)-lesioned parkinsonian rats led to behavioral recovery. Relative amphetamine-induced rotational behavior of 6-OHDA lesioned rats at baseline (before engraftment) and at 4, 8, and 12 weeks after intrastriatal transplantation of ITSCs cultured under standard conditions ($n = 7$) or pretreated with SHH/FGF8 ($n = 8$) and in sham-operated animals ($n = 5$). Baseline values were 12.9 $\pm$ 1.5 net rotations per minute for the sham animal group, 13.7 $\pm$ 0.5 for the standard-ITSC group, and 15.9 $\pm$ 3.8 for the pretreated-ITSC group ($F = 2.029$; $p = .156$, one-way analysis of variance [ANOVA]). Two-way repeated-measures ANOVA with post hoc t test and Bonferroni adjustment with time after transplantation as within-subject factor and treatment as between-subjects factor revealed a statistically significant main effect for time ($F[2.155, 38.781] = 10.947$, $p < .0001$; with Greenhouse-Geisser correction) and a statistically significant interaction effect of time and treatment ($F[4.309, 38.781] = 3.678$, $p = .011$). $*$, $p < .05$, $**$, $p < .01$, $***$, $p < .001$ when compared with pregraft baseline; + $p < .05$, ++ $p < .01$ when compared with sham control (post hoc Bonferroni adjusted t tests).

only a very small amount of TH^+ DA neurons was observable in the 6-OHDA-treated SN of the sham group (Fig. 5A, 5C; supplemental online Fig. 3). In contrast, transplantation of undifferentiated or SHH/FGF8-predifferentiated ITSCs into the ipsilateral striatum led to an increased amount of endogenous TH^+ DA neuron populations in the SN of the ipsilateral site (Fig. 5A, 5C; supplemental online Fig. 3). Anti-TH immunoreactivity within the striatum was unilaterally reduced in ipsilateral hemispheres. Remarkably, a slightly but significantly increased amount of incoming endogenous TH^+ fibers to the striatum could be observed in transplanted animals in contrast to sham controls, indicating recovered axonal sprouting through the nigrostriatal pathway or upregulation of TH in existing fibers (Fig. 5B, 5E).

We assessed potential associations of behavioral outcome measured by amphetamine-induced net rotations with ipsilateral and contralateral TH^+ DA neuron counts (Fig. 5F, 5G). No significant differences between undifferentiated and SHH/FGF8-predifferentiated ITSCs could be determined. Pearson correlation tests revealed a correlation with a magnitude >0.5 of ipsilateral net rotations after 12 weeks in percentage of pregraft rotations with log-transformed TH^+ cell counts on the ipsilateral side (Pearson correlation coefficient $r = -0.725$; $p = .027$) but not on the contralateral side ($r = 0.371$; $p = .325$).

ITSCs Integrate Into Parkinsonian Rat Brains and Give Rise to Neurons In Vivo

We assessed the role of ITSCs in recovering behavior and DA neuron populations of 6-OHDA-treated rats more closely by determining their survival in vivo at week 12 after transplantation. Using STEM121, a marker specific for human cytoplasm, we also ascertained whether ITSCs were capable of migrating from the striatal injection site to the lesioned SN. $STEM121^+$ ITSCs were primarily found to survive and migrate in loose streams toward the posterior direction (Fig. 6A, 6G, 6I). In only 1 of 10 analyzed animals, $STEM121^+$ ITSCs were clustered directly at the injection trajectory (Fig. 6B). Because of the injury, a large number of endogenous $GFAP^+$ reactive astrocytes were recruited to the injection site. STEM121/GFAP double immunolabeling exhibited differentiation of ITSCs into astrocytes in only very few cases (Fig. 6B). Most of the grafted cells that remained at the injection site appeared to retain the stem cell phenotype, as demonstrated by expression of the human-specific neural crest stem cell marker nestin (Fig. 6C). Because nestin-positive signals were found exclusively in cells closely located around the injection channel, these data indicate that grafts that migrated away from the injection site lost their stem cell characteristics 12 weeks after transplantation. Accordingly, ITSCs located at the respective target sites of migration lacked expression of Ki67, and we never observed formation of tumors in transplanted 6-OHDA rats (data not shown).

Investigating the role of ITSCs in recovering the parkinsonian phenotype in more detail, $STEM121^+$ ITSCs were shown to be located within the corpus callosum (Fig. 6E) and were consistently present within the midbrain (Fig. 6F–6H). Colabeling with STEM121 and the neuronal marker Map2 demonstrated the differentiation of ITSCs into neurons in vivo (Fig. 6D, 6H). Importantly, $STEM121^+/Map2^+$ ITSCs integrated directly above the lesioned SN (Fig. 6H). Next, we investigated whether grafted cells have the ability to adopt the DA phenotype. Interestingly, $STEM121^+/TH^+$ ITSCs were exclusively found within the locus ceruleus (Fig. 6I). Although ITSCs that integrated within the midbrain lacked TH expression, they ameliorated the functional outcome in parkinsonian rats, suggesting a trophic effect; therefore, they possess beneficial characteristics for recovering the parkinsonian phenotype.

Discussion

The present study describes for the first time that adult human neural crest-derived stem cells are capable of functionally recovering the nigrostriatal pathway of the unilaterally lesioned 6-OHDA PD rat model. Although 6-OHDA treatment does not induce the formation of Lewy bodies, in particular, the specific degeneration of nigral DA neurons and their striatal projections closely resembles the parkinsonian phenotype [3]. Linked to this neurodegenerative effect, unilaterally injected 6-OHDA is commonly known to cause rotational behavior in rats on administration of amphetamine [53, 54]. Given this close relation to the parkinsonian phenotype, the 6-OHDA rat model remains the state-of-the-art animal model in terms of evaluating the applicability of stem cell transplants for PD cell replacement therapy on both the behavioral and histological levels. We observed that the 6-OHDA-induced rotational behavior was significantly recovered by the intrastriatal transplantation of ITSCs independent of their predifferentiation, not by acquiring a DA phenotype within the SN or the striatum but most likely by restoring the endogenous nigrostriatal DA pathway.

Various rodent, primate, and human stem cell derivatives were shown to restore amphetamine-induced rotation behavior of 6-OHDA-lesioned rats by differentiating into DA neurons, such as pluripotent ESCs [17, 55, 56] and fetal neural progenitor

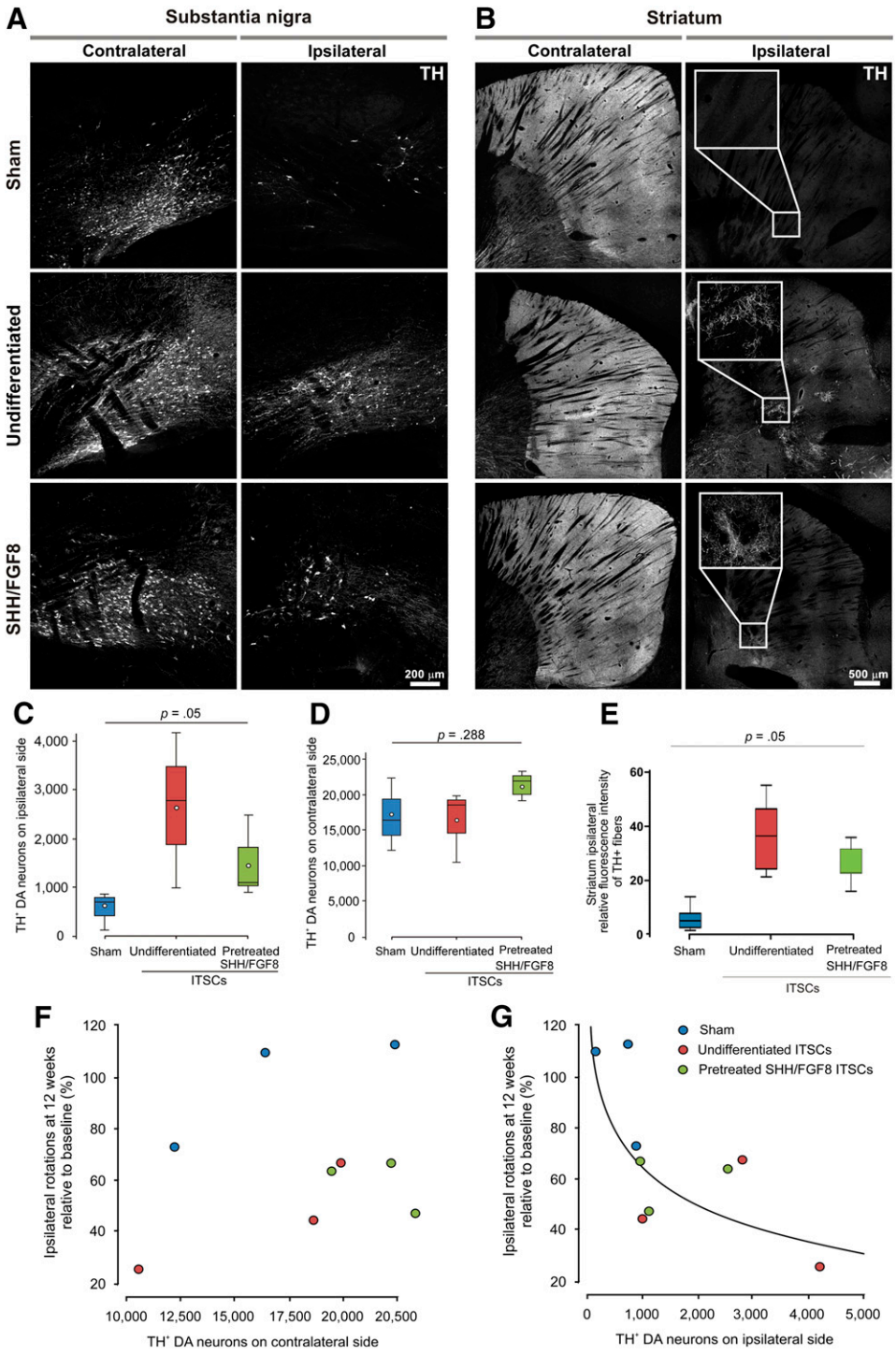

Figure 5. Lesioned substantia nigra (SN) of rats treated with 6-hydroxydopamine (6-OHDA) is restored after ITSC transplantation. **(A):** Contralateral hemispheres revealed normal endogenous populations of TH-positive DA neurons in the SN. Although almost no TH-expressing DA neurons were observable after transplantation of the sham group, populations of DA neurons were observable after transplantation of undifferentiated or predifferentiated ITSCs. **(B):** TH expression within the striatum contralateral and ipsilateral to an unilateral striatal 6-OHDA lesion 12 weeks after lesion. The 6-OHDA lesion affected TH^+ fibers only within the ipsilateral hemisphere. In contrast to the sham group, in transplanted animals, TH^+ fibers are clearly visible within the ipsilateral hemisphere (magnified view). **(C, D):** Box plots of TH^+ DA neuron counts in the SN on ipsilateral **(C)** and contralateral **(D)** sides with respect to the transplantation group, as measured by stereological analysis. The plots show the 10th percentile, 1st quartile, median, 3rd quartile, and 90th percentile for each parameter. Open circles represent the means. The *p* values are from one-way ANOVA according to Kruskal-Wallis. **(E):** Significantly increased amount of incoming endogenous TH+ fibers into ipsilateral striatum after transplantation of undifferentiated and SHH/FGF8-pretreated ITSCs in contrast to sham control. The *p* values are calculated by one-way ANOVA with post hoc Bonferroni-adjusted *t* test. **(F, G):** Correlations of ipsilateral amphetamine-induced rotations after 12 weeks with ipsilateral **(F)** and contralateral **(G)** TH^+ DA neuron counts. Values are means ± SEM. Abbreviations: DA, dopaminergic; ITSCs, adult human neural crest-derived stem cells derived from the inferior turbinate; TH, tyrosine hydroxylase.

cells [57]. Notably, ESC-derived DA-precursors even generated a complete recovery of 6-OHDA-induced rotational behavior 18 weeks after transplantation [15]. Overcoming ethical and practical considerations in terms of using embryonic tissue [16–18], induced pluripotent stem cells generated from adult somatic cells have also been described as efficiently generating DA neurons and restoring motor function after intrastriatal transplantation in PD animal models [58, 59].

In 2013, Reinhardt et al. showed that human small molecule neural progenitor cells derived from pluripotent stem cells were able to integrate into the SN and give rise to midbrain DA neurons in vivo only after predifferentiation with FGF8 and the SHH agonist purmorphamine [60]. As recently pioneered by Sieber-Blum and colleagues, treatment of neural crest-derived stem cells with FGF8 and SHH in combination with dual SMAD inhibition and inhibited WNT signaling (after a short activation period of WNT signaling for 1 day) resulted in their highly efficient differentiation into TH^+ dopaminergic neurons [45]. Applying the promising differentiation protocol described by Sieber-Blum and coworkers, we show successful differentiation of ITSCs into 100% Pitx3-positive dopaminergic progenitors, which further differentiated into TH^+ neurons after 20 days in vitro. However, ITSCs and their SHH/FGF8-predifferentiated derivatives did not show the DA phenotype within the striatum or after migration into the midbrain region near the SN at 12 weeks after transplantation. On the contrary, ITSCs acquired a TH^+ catecholaminergic phenotype after migrating into the locus ceruleus. This region is suggested to be critical in regulating the sensitivity of the nigrostriatal DA pathway in terms of PD [61]. Consequently, ITSC-derived DA neurons within the locus ceruleus may contribute in part to the behavioral recovery observed in this study.

Human MSCs have also been described to efficiently regenerate the parkinsonian phenotype in 6-OHDA-treated rats [62–64]. Notably, the observed recovery of rotational behavior after MSC transplantation was associated with secretion of paracrine factors rather than differentiation of MSCs into TH^+ DA neurons [62, 64, 65]. Linking these promising findings to primate models, Reymond and colleagues showed that transplantation of human neural stem cells leads to behavioral recovery of a primate PD model. Regenerative effects of transplanted neural stem cells (NSCs) were mainly associated with homeostatic adjustment of endogenous nigral DA neurons. In particular, some NSCs underwent differentiation into astrocyte-like cells expressing GDNF [66]. The presence of GDNF has been broadly shown to promote the recovery of parkinsonian phenotypes in different animal models [67–69]. Interestingly, human neural crest-derived stem cells from dental pulp were reported to provide neuroprotection for dopaminergic neurons in vitro by secreting various neurotrophic factors including GDNF, NGF, and BDNF [70]. Cotransplantation of neural crest-derived olfactory ensheathing cells (OECs) together with fetal ventral mesencephalic cells was further shown to restore functional deficits in a parkinsonian rat model. OECs supported the viability of cotransplanted fetal ventral mesencephalic cells [71], a matter closely related to their broadly described expression of neurotrophic factors like GDNF [72]. Notably, although residing exclusively within the middle and superior turbinate [73, 74] rather than in the inferior turbinate of the human nose, OECs are anatomically closely related to the ITSCs used in the present study [41].

Extending these promising findings on neural crest-derived cellular therapies in models of central nervous system disorders including PD, we showed that solely transplanted ITSCs are able to functionally recover a 6-OHDA-lesioned parkinsonian rat model. In accordance with the broad range of paracrine effects of adult stem cell transplants in terms of regenerating the parkinsonian phenotype [62, 66], we also observed significantly increased recovery of cell bodies of endogenous DA neurons within the SN and their projections into the striatum. The correlation of SN DA neuron counts on the ipsilateral side with the rotational behavior further indicates the trophic support provided by ITSCs to mediate the recovery effects of this transplantation approach. In addition, the site of ITSC migration within the midbrain and near the lesioned SN suggests an impact on the restoration of the lesioned substantia nigra via production of trophic factors. Considering the commonly described expression and secretion of GDNF, NGF or BDNF by mesenchymal stem cells [65, 75] and neural-crest-derived stem cells in vivo and in vitro [70, 72, 76], ITSCs may secrete similar neurotrophic factors to restore endogenous DA neuron populations—an interesting matter for more detailed investigation in future studies. Regarding their potential cellular source, endogenous TH^+ neurons observed after ITSC transplantation may be derived either by differentiation of neural progenitors closely located to the SN, such as ventral midbrain NSCs [77], via dedifferentiation of resident astrocytes [78] or by endogenous DA neurons that have not degenerated in the first place.

Analysis of whole brains in adjacent sections revealed another interesting finding: ITSCs migrate extensively from the injection trajectory in loose streams and primarily toward the posterior direction as far as the SN and the locus ceruleus. In accordance with the data presented, NCSCs have been reported previously as a highly migratory cell population that migrates in cell streams [79, 80]. However, such migratory properties of stem cells may also be associated with a potential risk of their tumorigenicity in clinical applications [81]. Although in 1 of 10 analyzed animals nonmigrating ITSCs located near the injection site expressed the progenitor marker nestin, we did not observe proliferating ITSCs at the respective target sites of migration, suggesting their low tumorigenic potential. In addition, ITSCs were reported not to form teratomas in immunodeficient SCID mice [41]. Consistent with these findings, NCSCs derived from the bulge of hair follicles were also shown not to undergo transformation after transplantation into a mouse model of spinal cord injury [33]. Accordingly, we never observed any signs of tumor formation in transplanted 6-OHDA-lesioned rats in the present study. In future studies, we will analyze transcriptomic profiles of ITSCs during dopaminergic differentiation. In conclusion, ITSCs seem to be a promising cell source for future therapeutic application in PD patients.

Conclusion

Our findings demonstrate the functional recovery of a 6-OHDA-treated PD rat model by transplantation of adult human neural crest-derived stem cells generated from the inferior turbinate. Due to their easy accessibility and the resulting possibility of an autologous transplantation approach, ITSCs represent a promising cell source for regenerative medicine. Given the observed enhanced migration capability of ITSCs within the parkinsonian rat brains, future transplantation strategies may also focus on intraventricular injection of ITSCs rather than their local application. Our study extends the variety of possible

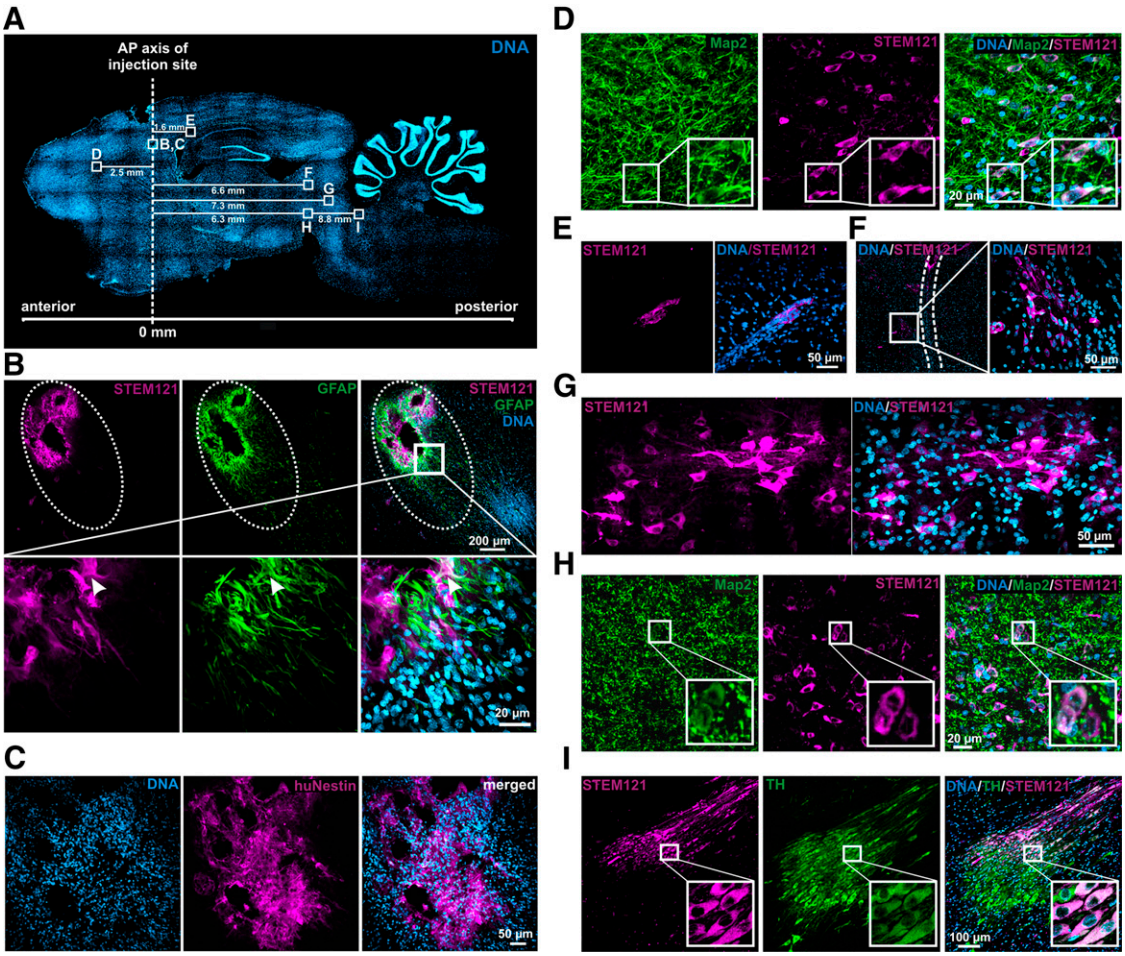

Figure 6. Adult human neural crest-derived stem cells derived from the inferior turbinate (ITSCs) survive and integrate into parkinsonian rat brains. Immunohistochemical analysis of sagittal 6-hydroxydopamine (6-OHDA) rat brain sections at 12 weeks after transplantation. **(A):** Whole-brain section stained with DAPI (4′,6-diamidino-2-phenylindole). Dotted line indicates AP axis of injection site. Squares depicting regions of interest with appropriate migration distances. **(B):** Cluster of STEM121$^+$ cells were directly located at the striatal injection site (upper panel). Dotted ellipse illustrates the injection channel. GFAP$^+$ astrocytes were recruited to the injury site. Magnified view: arrowhead indicates STEM121$^+$/GFAP$^+$ coexpressing cell (lower panel). **(C):** ITSCs remaining at the injection site kept their stem cell characteristics and expressed the human-specific neural crest stem cell marker nestin. **(D):** STEM121$^+$/Map2$^+$ ITSCs were shown to be located within the corpus callosum directly above the striatum. **(E):** At 12 weeks after transplantation, several STEM121$^+$ cells remained within the corpus callosum 1.6 mm posterior to the injection site. **(F):** In addition, STEM121$^+$ ITSCs were located adjacent to the injection channel of the 6-OHDA lesion, indicated by dotted lines **(G),** and 7.3 mm posterior to the striatal injection site within the midbrain. **(H):** STEM121$^+$/Map2$^+$ ITSCs integrated directly above the lesioned SN. **(I):** Stem121$^+$ ITSCs located in the locus ceruleus showed TH coexpression at the protein level, indicating their differentiation into DA neurons. Abbreviations: AP, anteroposterior; hNestin, human-specific neural crest stem cell marker nestin; TH, tyrosine hydroxylase.

applications of NCSCs within regenerative medicine, particularly emphasizing their great potential for future treatment of PD in the patient.

Acknowledgments

We thank Jared Sterneckert, Grit Weselek, and Andreas Hermann for helpful discussions on dopaminergic differentiation and quantitative histology. We thank Raphael Kurtz for advice on calcium imaging, Ulrike Schröder for valuable technical support, and Kyle J. Lauersen for critical reading. This work was supported by the Bundesministerium für Bildung und Forschung (research program "Gewinnung pluri- bzw. multipotenter Stammzellen", AZ: 01GN1006) to A.S., C.K., and B.K. C.O. was supported by a Gerok position from the DFG Collaborative Research Center 655, "Cells into tissues: stem cell and progenitor commitment and interactions during tissue formation." C.O. is currently affiliated with the Department of Neuropsychiatry and Laboratory of Molecular Psychiatry, Charité-Universitätsmedizin Berlin in Berlin, Germany. S.H. is currently affiliated with the German Center for Neurodegenerative Diseases in Tübingen, Germany, and the Department of Neurodegenerative Diseases, Hertie-Institute for Clinical Brain Research, Tübingen, Germany. D.W. is currently affiliated with the School of Pharmacy, University of Reading, Whiteknights, Reading, U.K.

Author Contributions

J.M.: collection and/or assembly of data, data analysis and interpretation, conception and design, manuscript writing, final approval of manuscript; C.O.: collection and/or assembly of

data, data analysis and interpretation, conception and design, final approval of manuscript; J.F.W.G.: data analysis and interpretation, manuscript writing, final approval of manuscript; S.H.: collection and/or assembly of data, final approval of manuscript; M.F.: collection and/or assembly of data; D.W. and C.K.: conception and design, data analysis and interpretation, final approval of manuscript; A.S.: conception and design, data analysis and interpretation, manuscript drafting and revision, financial support; B.K.: conception and design, data analysis and interpretation, final approval of manuscript, financial support.

Disclosure of Potential Conflicts of Interest

C.O. has compensated honoraria from UCB Pharma. M.F. has compensated honoraria from Meda Pharma and UCB Pharma, and compensated research funding from Deutsche Forschungsgemeinschaft. The other authors indicated no potential conflicts of interest.

References

1 Nussbaum RL, Ellis CE. Alzheimer's disease and Parkinson's disease. N Engl J Med 2003;348:1356–1364.

2 Corti O, Lesage S, Brice A. What genetics tells us about the causes and mechanisms of Parkinson's disease. Physiol Rev 2011;91:1161–1218.

3 Gray F. The neuropathology of Parkinson syndrome. Rev Neurol (Paris) 1988 144:229–248; [in French] [PubMed].

4 Cotzias GC, Van Woert MH, Schiffer LM. Aromatic amino acids and modification of parkinsonism. N Engl J Med 1967;276:374–379.

5 Krack P, Batir A, Van Blercom N et al. Five-year follow-up of bilateral stimulation of the subthalamic nucleus in advanced Parkinson's disease. N Engl J Med 2003;349:1925–1934.

6 Wolz M, Hauschild J, Koy J et al. Immediate effects of deep brain stimulation of the subthalamic nucleus on nonmotor symptoms in Parkinson's disease. Parkinsonism Relat Disord 2012;18:994–997.

7 Love S, Plaha P, Patel NK et al. Glial cell line-derived neurotrophic factor induces neuronal sprouting in human brain. Nat Med 2005;11:703–704.

8 Kaplitt MG, Feigin A, Tang C et al. Safety and tolerability of gene therapy with an adeno-associated virus (AAV) borne GAD gene for Parkinson's disease: An open label, phase I trial. Lancet 2007;369:2097–2105.

9 Fabbrini G, Brotchie JM, Grandas F et al. Levodopa-induced dyskinesias. Mov Disord 2007;22:1379–1389; quiz 1523.

10 Fahn S. Does levodopa slow or hasten the rate of progression of Parkinson's disease? J Neurol 2005;252(suppl 4):IV37–IV42.

11 Lindvall O, Brundin P, Widner H et al. Grafts of fetal dopamine neurons survive and improve motor function in Parkinson's disease. Science 1990;247:574–577.

12 Freed CR, Breeze RE, Rosenberg NL et al. Survival of implanted fetal dopamine cells and neurologic improvement 12 to 46 months after transplantation for Parkinson's disease. N Engl J Med 1992;327:1549–1555.

13 Spencer DD, Robbins RJ, Naftolin F et al. Unilateral transplantation of human fetal mesencephalic tissue into the caudate nucleus of patients with Parkinson's disease. N Engl J Med 1992;327:1541–1548.

14 Freed CR, Greene PE, Breeze RE et al. Transplantation of embryonic dopamine neurons for severe Parkinson's disease. N Engl J Med 2001;344:710–719.

15 Kriks S, Shim JW, Piao J et al. Dopamine neurons derived from human ES cells efficiently engraft in animal models of Parkinson's disease. Nature 2011;480:547–551.

16 Erdö F, Bührle C, Blunk J et al. Host-dependent tumorigenesis of embryonic stem cell transplantation in experimental stroke. J Cereb Blood Flow Metab 2003;23:780–785.

17 Brederlau A, Correia AS, Anisimov SV et al. Transplantation of human embryonic stem cell-derived cells to a rat model of Parkinson's disease: Effect of in vitro differentiation on graft survival and teratoma formation. Stem Cells 2006;24:1433–1440.

18 Ben-Porath I, Thomson MW, Carey VJ et al. An embryonic stem cell-like gene expression signature in poorly differentiated aggressive human tumors. Nat Genet 2008;40:499–507.

19 Blum B, Benvenisty N. The tumorigenicity of human embryonic stem cells. Adv Cancer Res 2008;100:133–158.

20 Wagers AJ, Weissman IL. Plasticity of adult stem cells. Cell 2004;116:639–648.

21 Ben-David U, Benvenisty N. The tumorigenicity of human embryonic and induced pluripotent stem cells. Nat Rev Cancer 2011;11:268–277.

22 Ra JC, Shin IS, Kim SH et al. Safety of intravenous infusion of human adipose tissue-derived mesenchymal stem cells in animals and humans. Stem Cells Dev 2011;20:1297–1308.

23 Wakitani S, Mitsuoka T, Nakamura N et al. Autologous bone marrow stromal cell transplantation for repair of full-thickness articular cartilage defects in human patellae: Two case reports. Cell Transplant 2004;13:595–600.

24 Kitoh H, Kitakoji T, Tsuchiya H et al. Transplantation of culture expanded bone marrow cells and platelet rich plasma in distraction osteogenesis of the long bones. Bone 2007;40:522–528.

25 Bonab MM, Sahraian MA, Aghsaie A et al. Autologous mesenchymal stem cell therapy in progressive multiple sclerosis: An open label study. Curr Stem Cell Res Ther 2012;7:407–414.

26 Schiavetta A, Maione C, Botti C et al. A phase II trial of autologous transplantation of bone marrow stem cells for critical limb ischemia: Results of the Naples and Pietra Ligure Evaluation of Stem Cells study. Stem Cells Translational Medicine 2012;1:572–578.

27 Wang Y, Yang J, Li H et al. Hypoxia promotes dopaminergic differentiation of mesenchymal stem cells and shows benefits for transplantation in a rat model of Parkinson's disease. PLoS One 2013;8:e54296.

28 Barzilay R, Kan I, Ben-Zur T et al. Induction of human mesenchymal stem cells into dopamine-producing cells with different differentiation protocols. Stem Cells Dev 2008;17:547–554.

29 Trzaska KA, Rameshwar P. Dopaminergic neuronal differentiation protocol for human mesenchymal stem cells. Methods Mol Biol 2011;698:295–303.

30 Franco Lambert AP, Fraga Zandonai A, Bonatto D et al. Differentiation of human adipose-derived adult stem cells into neuronal tissue: Does it work? Differentiation 2009;77:221–228.

31 Toma JG, Akhavan M, Fernandes KJ et al. Isolation of multipotent adult stem cells from the dermis of mammalian skin. Nat Cell Biol 2001;3:778–784.

32 Sieber-Blum M, Grim M, Hu YF et al. Pluripotent neural crest stem cells in the adult hair follicle. Dev Dyn 2004;231:258–269.

33 Sieber-Blum M, Schnell L, Grim M et al. Characterization of epidermal neural crest stem cell (EPI-NCSC) grafts in the lesioned spinal cord. Mol Cell Neurosci 2006;32:67–81.

34 Widera D, Zander C, Heidbreder M et al. Adult palatum as a novel source of neural crest-related stem cells. Stem Cells 2009;27:1899–1910.

35 Davies LC, Locke M, Webb RD et al. A multipotent neural crest-derived progenitor cell population is resident within the oral mucosa lamina propria. Stem Cells Dev 2010;19:819–830.

36 Marynka-Kalmani K, Treves S, Yafee M et al. The lamina propria of adult human oral mucosa harbors a novel stem cell population. Stem Cells 2010;28:984–995.

37 Seo BM, Miura M, Gronthos S et al. Investigation of multipotent postnatal stem cells from human periodontal ligament. Lancet 2004;364:149–155.

38 Widera D, Grimm WD, Moebius JM et al. Highly efficient neural differentiation of human somatic stem cells, isolated by minimally invasive periodontal surgery. Stem Cells Dev 2007;16:447–460.

39 Kaltschmidt B, Kaltschmidt C, Widera D. Adult craniofacial stem cells: Sources and relation to the neural crest. Stem Cell Rev 2012;8:658–671.

40 Greiner JF, Hauser S, Widera D et al. Efficient animal-serum free 3D cultivation method for adult human neural crest-derived stem cell therapeutics. Eur Cell Mater 2011;22:403–419.

41 Hauser S, Widera D, Qunneis F et al. Isolation of novel multipotent neural crest-derived stem cells from adult human inferior turbinate. Stem Cells Dev 2012;21:742–756.

42 Greiner JF, Grunwald LM, Müller J et al. Culture bag systems for clinical applications of adult human neural crest-derived stem cells. Stem Cell Res Ther 2014;5:34.

43 Hunt DP, Morris PN, Sterling J et al. A highly enriched niche of precursor cells with neuronal and glial potential within the hair follicle dermal papilla of adult skin. Stem Cells 2008;26:163–172.

44 Kubo A, Yoshida T, Kobayashi N et al. Efficient generation of dopamine neuron-like

cells from skin-derived precursors with a synthetic peptide derived from von Hippel-Lindau protein. Stem Cells Dev 2009;18:1523–1532.

45 Narytnyk A, Verdon B, Loughney A et al. Differentiation of human epidermal neural crest stem cells (hEPI-NCSC) into virtually homogenous populations of dopaminergic neurons. Stem Cell Rev 2014;10:316–326.

46 Betarbet R, Sherer TB, Greenamyre JT. Animal models of Parkinson's disease. BioEssays 2002;24:308–318.

47 Kehinde LO, Buraimoh-Igbo LA, Ude OU et al. Electronic rotameter for quantitative evaluation of rotational behaviour in rats after unilateral lesions of the nigrostriatal dopamine system. Med Biol Eng Comput 1984;22:361–366.

48 Robinson TE, Becker JB. The rotational behavior model: Asymmetry in the effects of unilateral 6-OHDA lesions of the substantia nigra in rats. Brain Res 1983;264:127–131.

49 Hermann A, Loewenbrück KF, Boldt Ä et al. Lack of vascular endothelial growth factor receptor-2/Flk1 signaling does not affect substantia nigra development. Neurosci Lett 2013;553:142–147.

50 Schneider CA, Rasband WS, Eliceiri KW. NIH Image to ImageJ: 25 years of image analysis. Nat Methods 2012;9:671–675.

51 Hynes M, Porter JA, Chiang C et al. Induction of midbrain dopaminergic neurons by Sonic hedgehog. Neuron 1995;15:35–44.

52 Wang MZ, Jin P, Bumcrot DA et al. Induction of dopaminergic neuron phenotype in the midbrain by Sonic hedgehog protein. Nat Med 1995;1:1184–1188.

53 Hefti F, Melamed E, Wurtman RJ. Partial lesions of the dopaminergic nigrostriatal system in rat brain: Biochemical characterization. Brain Res 1980;195:123–137.

54 Schober A. Classic toxin-induced animal models of Parkinson's disease: 6-OHDA and MPTP. Cell Tissue Res 2004;318:215–224.

55 Bjorklund LM, Sánchez-Pernaute R, Chung S et al. Embryonic stem cells develop into functional dopaminergic neurons after transplantation in a Parkinson rat model. Proc Natl Acad Sci USA 2002;99:2344–2349.

56 Baier PC, Schindehütte J, Thinyane K et al. Behavioral changes in unilaterally 6-hydroxydopamine lesioned rats after transplantation of differentiated mouse embryonic stem cells without morphological integration. STEM CELLS 2004;22:396–404.

57 Schwarz SC, Wittlinger J, Schober R et al. Transplantation of human neural precursor cells in the 6-OHDA lesioned rats: Effect of immunosuppression with cyclosporine A. Parkinsonism Relat Disord 2006;12:302–308.

58 Sundberg M, Bogetofte H, Lawson T et al. Improved cell therapy protocols for Parkinson's disease based on differentiation efficiency and safety of hESC-, hiPSC-, and non-human primate iPSC-derived dopaminergic neurons. STEM CELLS 2013;31:1548–1562.

59 Hargus G, Cooper O, Deleidi M et al. Differentiated Parkinson patient-derived induced pluripotent stem cells grow in the adult rodent brain and reduce motor asymmetry in parkinsonian rats. Proc Natl Acad Sci USA 2010;107:15921–15926.

60 Reinhardt P, Glatza M, Hemmer K et al. Derivation and expansion using only small molecules of human neural progenitors for neurodegenerative disease modeling. PLoS One 2013;8:e59252.

61 Gesi M, Soldani P, Giorgi FS et al. The role of the locus coeruleus in the development of Parkinson's disease. Neurosci Biobehav Rev 2000;24:655–668.

62 Cova L, Armentero MT, Zennaro E et al. Multiple neurogenic and neurorescue effects of human mesenchymal stem cell after transplantation in an experimental model of Parkinson's disease. Brain Res 2010;1311:12–27.

63 Pavón-Fuentes N, Blanco-Lezcano L, Martínez-Martín L et al. Stromal cell transplant in the 6-OHDA lesion model. Rev Neurol 2004 39:326–334; [in Spanish] [PubMed].

64 Blandini F, Cova L, Armentero MT et al. Transplantation of undifferentiated human mesenchymal stem cells protects against 6-hydroxydopamine neurotoxicity in the rat. Cell Transplant 2010;19:203–217.

65 Glavaski-Joksimovic A, Bohn MC. Mesenchymal stem cells and neuroregeneration in Parkinson's disease. Exp Neurol 2013;247:25–38.

66 Redmond DE Jr., Bjugstad KB, Teng YD et al. Behavioral improvement in a primate Parkinson's model is associated with multiple homeostatic effects of human neural stem cells. Proc Natl Acad Sci USA 2007;104:12175–12180.

67 Kordower JH, Emborg ME, Bloch J et al. Neurodegeneration prevented by lentiviral vector delivery of GDNF in primate models of Parkinson's disease. Science 2000;290:767–773.

68 Gash DM, Zhang Z, Ovadia A et al. Functional recovery in parkinsonian monkeys treated with GDNF. Nature 1996;380:252–255.

69 Bilang-Bleuel A, Revah F, Colin P et al. Intrastriatal injection of an adenoviral vector expressing glial-cell-line-derived neurotrophic factor prevents dopaminergic neuron degeneration and behavioral impairment in a rat model of Parkinson disease. Proc Natl Acad Sci USA 1997;94:8818–8823.

70 Nosrat IV, Smith CA, Mullally P et al. Dental pulp cells provide neurotrophic support for dopaminergic neurons and differentiate into neurons in vitro; implications for tissue engineering and repair in the nervous system. Eur J Neurosci 2004;19:2388–2398.

71 Agrawal AK, Shukla S, Chaturvedi RK et al. Olfactory ensheathing cell transplantation restores functional deficits in rat model of Parkinson's disease: A cotransplantation approach with fetal ventral mesencephalic cells. Neurobiol Dis 2004;16:516–526.

72 Woodhall E, West AK, Chuah MI. Cultured olfactory ensheathing cells express nerve growth factor, brain-derived neurotrophic factor, glia cell line-derived neurotrophic factor and their receptors. Brain Res Mol Brain Res 2001;88:203–213.

73 Murrell W, Feron F, Wetzig A et al. Multipotent stem cells from adult olfactory mucosa. Dev Dyn 2005;233:496–515.

74 Mackay-Sim A. Stem cells and their niche in the adult olfactory mucosa. Arch Ital Biol 2010;148:47–58.

75 Chen X, Katakowski M, Li Y et al. Human bone marrow stromal cell cultures conditioned by traumatic brain tissue extracts: Growth factor production. J Neurosci Res 2002;69:687–691.

76 Ganz J, Arie I, Ben-Zur T et al. Astrocyte-like cells derived from human oral mucosa stem cells provide neuroprotection in vitro and in vivo. STEM CELLS TRANSLATIONAL MEDICINE 2014;3:375–386.

77 Hegarty SV, Spitere K, Sullivan AM et al. Ventral midbrain neural stem cells have delayed neurogenic potential in vitro. Neurosci Lett 2014;559:193–198.

78 Wachter B, Schürger S, Rolinger J et al. Effect of 6-hydroxydopamine (6-OHDA) on proliferation of glial cells in the rat cortex and striatum: Evidence for de-differentiation of resident astrocytes. Cell Tissue Res 2010;342: 147–160.

79 Mayor R, Theveneau E. The role of the non-canonical Wnt-planar cell polarity pathway in neural crest migration. Biochem J 2014;457: 19–26.

80 Takahashi Y, Sipp D, Enomoto H. Tissue interactions in neural crest cell development and disease. Science 2013;341:860–863.

81 Jeong JO, Han JW, Kim JM et al. Malignant tumor formation after transplantation of short-term cultured bone marrow mesenchymal stem cells in experimental myocardial infarction and diabetic neuropathy. Circ Res 2011;108:1340–1347.

See www.StemCellsTM.com for supporting information available online.

